Supplementary materials: A comprehensive framework for assessing the accuracy and uncertainty of global above-ground biomass maps

Table S1. Metadata of the plot dataset.

ID	Scale	Type	Count	Avg. year	inventory	Avg. size (ha)	Avg. AGB (Mg ha -1)	Dominant biome	Reference
AFR2	Regional	Research plot	593	2007		0.69	118.51	Tropical rainforest	Lindsell and Klop (2013)
AFR4	Local	Research plot	110	2005		0.25	13.72	Tropical mountain system	De Vries et al. (2012)
AFR5	Local	Research plot	71	2008		0.16	118.6	Tropical rainforest	Laurin et al. (2016)
AFR6	Local	Research plot	24	2008		0.54	358.85	Tropical rainforest	Willcock et al. (2014)
AFR7	Local	Research plot**	19	2008		0.64	32.58	Tropical rainforest	Lewis et al. (2013)
AFR8	National	NFI	105	2010		0.25	187.67	Tropical moist forest	Carreiras et al. (2012)
AFR9	Local	Research plot	41	2006		0.12	164.16	Tropical dry forest	Carreiras et al. (2013)
AFR10	Local	Research plot	18	2012		0.13	216.29	Tropical rainforest	Mitchard et al. (2011)
AFR11	National	NBS*	726	2012		0.08	266.36	Tropical rainforest	Drichi (2003); Avitabile et al. (2012)
AFR12	National	NFI	108	2009		0.67	371.28	Tropical rainforest	Avitabile et al. (2012)
AFR13	Local	Research plot	25	2012		1	243.52	Tropical rainforest	Mitchard et al. (2009)
AFR14	Local	Research plot	88	2008		0.13	70.37	Tropical dry forest	Mitchard et al. (2009)
AFR15	National	NFI	680	2011		0.13	25.35	Tropical mountain system	Vieilledent et al. (2016)
AFR FOS	Regional	Research plot**	527	2013		0.44	287.77	Tropical rainforest	Schepaschenko et al. (2019)
ASI CH	National	NFI	1267	2008		0.1	129.39	Subtropical mountain system	Zhang et al. (2019)
ASI FOS	Local	Research plot	15	2006		0.4	308.6	Tropical rainforest	Schepaschenko et al. (2019)
ASI IND	Local	Research plot	96	1996		1	272.43	Tropical rainforest	Ramesh et al. (2010)
ASI PH	National	NFI	1210	2004		0.43	58.04	Tropical rainforest	Araza et al. (2021)
ASI1	Regional	NFI	2903	2008		0.05	108.19	Tropical mountain system and rainforest	Avitabile et al. (2016)
ASI2	Local	Research plot	119	2011		0.11	181.03	Tropical dry forest	WWF and OBf, 2013
ASI3	Local	Research plot	92	2007		1	163.45	Tropical rainforest	Morel et al. (2011)
ASI4	Local	Research plot	70	2010		0.02	208.48	Tropical dry forest	Wijaya et al. (2015)
ASI5	Local	Research plot	28	2015		3.07	35.93	Tropical rainforest	Slik et al. (2013)
ASI8	Local	Research plot	31	2008		0.02	304.81	Tropical dry forest	Murdiyarso et al. (2009)
ASI9	Regional	Research plot	74	2012		0.13	309.16	Tropical rainforest	Avitabile et al. (2016)
AUS FOS	Local	Research plot	3	2004		0.68	168.37	Tropical dry forest	Schepaschenko et al. (2019)
AUS INJ	National	NFI	5001	2000		0.25	76.66	Subtropical steppe	Tickle et al. 2016
AUS1	National	NFI	9113	2008		0.13	268.57	Tropical dry forest	Auscover (2016)
CAM FOS	Local	Research plot	19	2012		0.97	248.66	Tropical rainforest	Schepaschenko et al. (2019)
CAM1	National	NFI	4045	2006		0.16	82.3	Tropical dry/moist/rain forest	de Jong (2013)
EU FOS	Regional	Research plot	170	2014		0.27	194.02	Boreal coniferous forest	Schepaschenko et al. (2019)
EU1	National	NFI	16819	2011		0.01	76.37	Temperate broadleaf and Boreal forests	NA
EU2	National	NFI	58185	2003		0.2	60.45	Mediterranean forests	NA
EU3	National	NFI	3021	2013		0.06	190.98	Temperate oceanic forest	Schelhaas et al. (2014)
EU4	National	NFI	5967	2007		0.06	176.07	Temperate broadleaf and Mediterranean forests	NA
NAM1	National	NFI	588	2010		0.04	96.01	Boreal coniferous forest	Liang et al. (2015)
NAM2	Local	Research plot	75	2004		0.04	293.55	Temperate mountain system	Luyssaert et al. (2008)
NAM3	Regional	NFI	586	2010		0.03	130.93	Temperate continental forest	NA
NAM4	Regional	NFI	2798	2010		0.04	79.42	Temperate continental forest	NA
SAM FOS	Regional	Research plot**	161	2010		0.47	333.25	Tropical rainforest	Schepaschenko et al. (2019); Mitchard et al. (2014)
SAM2	National	Research plot**	281	2013		0.34	208.65	Tropical rainforest	dos Santos et al. (2019)
SAM3	National	NFMS***	111	2011		0.13	395.3	Tropical rainforest	Brown et al. (2014)
SAM4	Local	Research plot	7	2014		0.15	352.51	Tropical rainforest	Goodman et al. (2013)
SAM5	Local	Research plot	23	2014		0.6	144.11	Tropical rainforest	NA
SAM TAP	Local	Research plot	46	2009		0.25	217.71	Tropical rainforest	Bispo et al. (2014)
SAM BAJO	Local	Research plot	122	2017		0.26	74.52	Tropical rainforest	Pacheco-Pascagaza et al. (2018)

*National Biomass System and ***National Forest Monitoring System, both comparable to NFIs; **Include key long-term sites supported by the Amazon Forest Inventory Network (RAINFOR) and African Tropical Rainforest Observatory Network (AfriTRON).

Table S2. Summary statistics of plot data per major climatic zone and continent used for 2000, 2008/10, and 2017 map comparisons, respectively.

Major climatic zone and continent	Plot (n)	Avg. year	Avg. size $\pm SD(ha)$	Avg. AGB (min. - max) (Mg ha^{-1})
Boreal	**5783**	**2008.5**	**0.02 ±0.06**	**56.4 (0 - 360.4)**
Europe	5443	2008.5	0.02 ±0.06	54.1 (0 - 360.4)
N.America	340	2009.0	0.04 ±0	93.3 (0.1 - 247.2)
Subtropical	**56880**	**2003.4**	**0.19 ±0.04**	**55.8 (0 - 1212.5)**
Asia	1149	2008.0	0.1 ±0	114.6 (0.3 - 691.5)
Australia	3938	2001.8	0.2 ±0.1	113 (0 - 1212.5)
C.America	50	2006.0	0.16 ±0	50.8 (0.4 - 223)
Europe	51743	2003.6	0.19 ±0.02	45.2 (0 - 629.3)
Temperate	**17892**	**2005.8**	**0.11 ±0.08**	**133.8 (0 - 5676.1)**
Australia	1223	2007.4	0.08 ±0.04	298.4 (0.5 - 5676.1)
Europe	14480	2005.1	0.12 ±0.08	129.3 (0 - 973)
N.America	2189	2008.9	0.04 ±0.02	71.1 (0 - 937.1)
Tropical	**12307**	**2006.8**	**0.22 ± 0.42**	**109.7 (0 - 869.8)**
Africa	3534	2007.5	0.3 ±0.19	150.3 (0 - 863.1)
Asia	3900	2006.9	0.17 ±0.23	84.5 (0 - 830.9)
Australia	238	2005.3	0.32 ±1.62	31 (0 - 238.5)
C.America	3990	2006.0	0.16 ±0	67.3 (0 - 859.2)
S.America	645	2008.8	0.46 ±1.33	330.6 (18 - 869.8)

Major climatic zone and continent	Plot (n)	Avg. year	Avg. size $\pm SD(ha)$	Avg. AGB (min. - max) (Mg ha^{-1})
Boreal	**11865**	**2010.6**	**0.02 ±0.05**	**67.7 (0 - 429.4)**
Europe	11289	2010.6	0.02 ±0.05	66.2 (0 - 429.4)
N.America	576	2010	0.04 ±0.01	97.1 (0.2 - 273.4)
Subtropical	**63297**	**2003.7**	**0.19 ±0.05**	**79.6 (0 - 2096.4)**
Asia	1268	2008	0.1 ±0.01	131.5 (7.9 - 691.5)
Australia	9746	2003.2	0.19 ±0.11	138.4 (0 - 2096.4)
C.America	51	2006	0.16 ±0.01	70.3 (11.3 - 223)
Europe	52232	2003.6	0.19 ±0.02	67.4 (7.2 - 647.3)
Temperate	**26674**	**2008**	**0.09 ±0.12**	**179.9 (0.1 - 6822.4)**
Australia	2978	2010.7	0.08 ±0.1	475.9 (0.3 - 6822.4)
Europe	20290	2007.3	0.1 ±0.14	147.8 (0.2 - 1071.2)
N.America	3406	2009.8	0.04 ±0.02	93.2 (0.1 - 937.1)
Tropical	**14345**	**2007.4**	**0.25 ± 0.51**	**150.2 (0 - 1268.8)**
Africa	4285	2008.4	0.31 ±0.43	191.7 (0 - 980.6)
Asia	4449	2006.7	0.21 ±0.39	118.1 (2.1 - 1268.8)
Australia	316	2006.9	0.29 ±1.41	53.4 (0 - 276.2)
C.America	4006	2006	0.16 ±0.06	98.8 (16.2 - 865.2)
S.America	1289	2010.7	0.41 ±1.07	306.9 (1.5 - 876.8)

Major climatic zone and continent	Plot (n)	Avg. year	Avg. size $\pm SD(ha)$	Avg. AGB (min. - max) (Mg ha^{-1})
Boreal	**11661**	**2010.6**	**0.02 ±0.03**	**74.8 (3.7 - 437.1)**
Europe	11088	2010.6	0.02 ±0.03	73.3 (3.7 - 437.1)
N.America	573	2010.0	0.04 ±0	104.8 (7 - 281.9)
Subtropical	**21004**	**2006.8**	**0.18 ±0.06**	**101.9 (8.6 - 2103.4)**
Asia	1149	2008.0	0.1 ±0	136.4 (25.4 - 691.5)
Australia	2472	2009.7	0.14 ±0.15	186 (8.6 - 2103.4)
C.America	50	2006.0	0.16 ±0	83.9 (28.8 - 223)
Europe	17333	2006.3	0.19 ±0.04	87.7 (25.4 - 651.9)
Temperate	**20889**	**2009.6**	**0.06 ±0.13**	**204.7 (7.3 - 6823.9)**
Australia	2716	2011.3	0.08 ±0.1	519.8 (12.8 - 6823.9)
Europe	14970	2009.1	0.07 ±0.14	168.7 (7.3 - 1080.4)
N.America	3203	2010.0	0.04 ±0.01	105.8 (16 - 465.8)
Tropical	**11545**	**2008.1**	**0.22 ± 0.5**	**181.3 (7 - 991.5)**
Africa	3395	2009.2	0.32 ±0.22	234.1 (7 - 991.5)
Asia	3113	2008.2	0.09 ±0.4	139.3 (25.9 - 703.3)
Australia	217	2008.7	0.3 ±1.7	70.4 (20.4 - 283)
C.America	3609	2006.0	0.16 ±0.06	125.8 (43.5 - 862.8)
S.America	1211	2010.6	0.4 ±1.08	326.5 (27.1 - 883.8)

Table S3. List of global and pantropical biomass maps epoch 2000 onwards.

AGB map	Spatial scale	Forest mask data	Pixel size	Epoch	RS and in situ data	Open access (OA)	OA uncertainty layer	Reference
Avitabile	pantropical	-	1km	2000-2008	Fusion of Saatchi and Baccini Pantropical	Yes	Yes	Avitabile et al. (2016)
Baccini Global	global	GLAS data and tree canopy cover thresholds	30m	2000	GLAS, MODIS, SRTM	Yes	Yes[1]	GlobalForestWatch (2002)
Baccini Pantropical	pantropical	-	1km	2007-2008	GLAS, MODIS, SRTM	Yes	Yes	Baccini et al. (2012)
Chen	global	GLC2000 forest and VCF threshold	1km	2007-2008	MODIS-NBAR	No	No	Chen et al. (2018)
CCI Biomass	global	-	100m	2017	ALOS2 PALSAR2, Sentinel 1	Yes	Yes	Santoro and Cartus (2019)
Hu	global	MODIS Land Cover	1km	2004	GLAS, MODIS, SRTM	No	No	Hu et al. (2016)
Kindermann	global	FRA forest area	55km	2005	FAO statistics, modelled NPP	No	No	Kindermann et al. (2008)
Liu	global	MODIS Land Cover forest	27.5km	1993-2012	L-VOD	No	No	Liu et al. (2015)
GEOCARBON	global	GLC2000 forests	1km	2007-2010	Fusion of Avitabile and Santoro	Yes	Yes	Avitabile et al. (2014); Santoro et al. (2015)
GlobBiomass	global	-	100m	2010	ALOS-PALSAR, ENVISAT, ASAR	Yes	Yes	Santoro et al. (2020)
Ruesch-Gibbs	global	GLC2000 forests	1km	2000	GLC2000, IPCC data	No	No	Ruesch and Gibbs (2008)
Saatchi	pantropical	-	1km	2000	GLAS, MODIS, QSCAT, SRTM, forest plots	No	No	Saatchi et al. (2011)
Yang	global	Per continent based on secondary data	1km	2005	VCF, GLASS LAI, forest plots, regional maps	No	No	Yang et al. (2020)
Zhang	global	GFC tree cover threshold	1km	2000	Fusion of local and global maps	No	No	Zhang and Liang (2020)

[1] Currently accessible at Google Earth Engine (https://code.earthengine.google.com/11b2fe70fd7019cd70fafa375bb3a525),but will be re-uploaded to its original repository at global forest watch platform.

Fig. S1. Comparison of the assessments when using the grid cells from the current approach and after strict filtering to mitigate preferential sampling. The latter involved the following steps: (1) Use of the plot dataset used to assess the 2010 GlobBiomass map, and the 30-m Hansen 2010 tree cover (TC) as a proxy for AGB variability (Avitabile and Camia, 2018). (2) Compute the mean TC of the grid cell and at plot locations, and their difference (mean plot TC − mean grid cell TC). The standard error of the mean TC at plot locations is also computed. Assuming the difference is normally distributed, a grid cell is accepted if the mean of the exhaustively sampled TC is within the 90% confidence interval of the true mean TC. (3) Assess the effect of preferential sampling through GlobBiomass assessments using grid cells from strict filter and the current approach. The slight differences between the two comparisons, even for the >300 Mg ha^{-1} bins, indicate that preferential sampling is unlikely to have much impact on our analysis. This can be attributed to our use of more NFIs than research plots and the fact that many of the research plots used are within forests which visually exhibit homogeneous canopy cover.

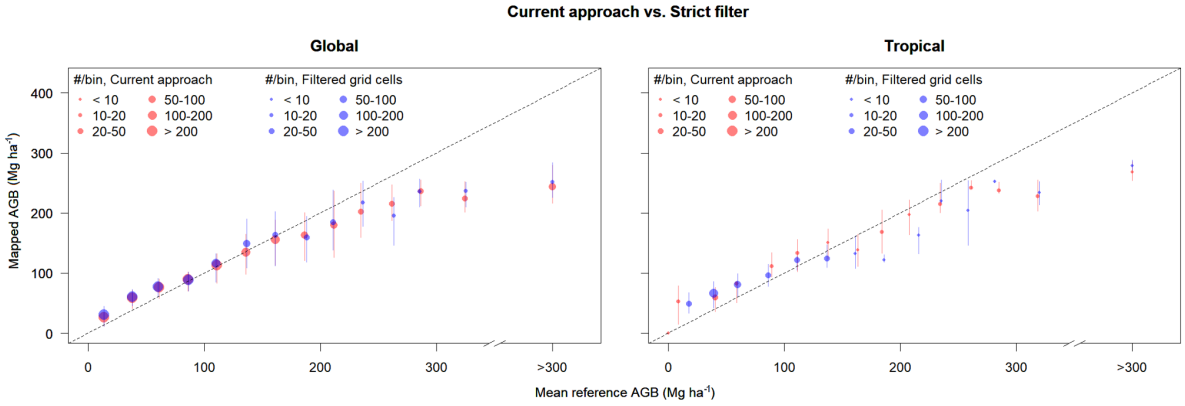

Fig. S2. Locations of all possible pantropical grid cells and those selected under both the current approach and strict filtering in high AGB tropical areas wherein 77% of the grid cells chosen under the current approach are also chosen after strict filtering. The average number of plots inside selected 0.1° grid cells is 10.89 for the current approach and 11.59 for the strict filter.

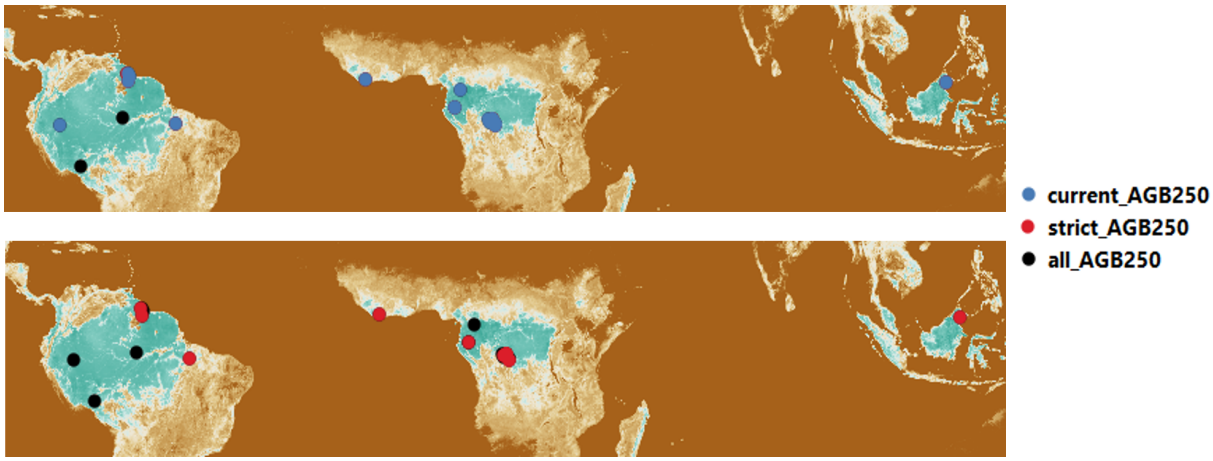

Table S4. Summary results for the weighted RF models used for bias modelling with the explained trend (%) and the rank and percentage of the Variable Importance Measure (VIM) values per covariate. The covariates in the Baccini model exclude the SD layer (currently only available for the pantropics) to enable global bias prediction.

RF model	Explained trend (%)	VIM rank	VIM proportion (%)
Baccini	36	Above-ground Biomass map (AGB), Tree Cover (TC), Slope (SL), Aspect (ASP)	49,32,12,7
GEOCARBON	24	AGB, TC, Standard Deviation layer (SD), SL, ASP	30,27,17,15,11
GlobBiomass	27	TC, AGB, SD, SLP, ASP	27,26,19,17,11
CCI Biomass	33	AGB, TC, SD, SL, ASP	26,22,19,17,17

Fig. S3. Partial Dependence Plots of predicted bias as a function of a covariate pair in the CCI Biomass map: (a) AGB map and tree cover at 0.1° ; and (b) slope and aspect at original map pixel size of 100 m.

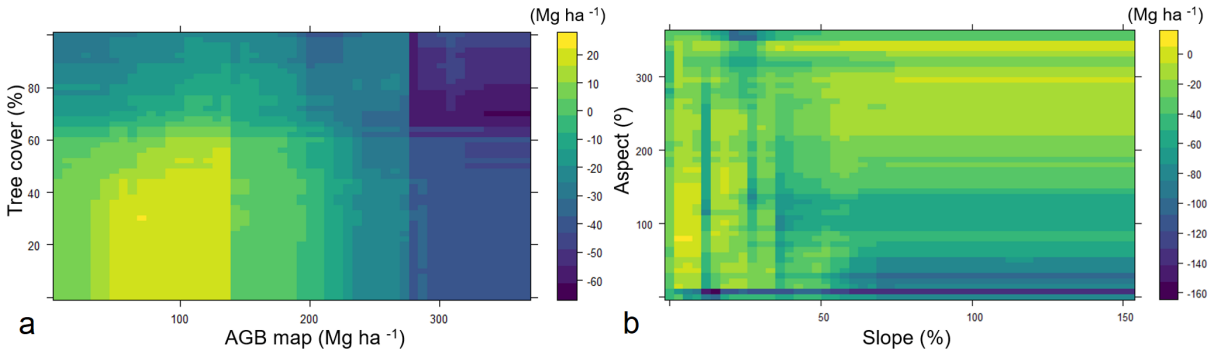

Fig. S4. Plot-to-map comparison for the bias-corrected AGB maps indicating an increase in map accuracy (relative to Fig. 4). The comparisons used a third of the total grid cells, independent to the ones used for the bias modelling: Baccini=2187, GEOCARBON=2174, GlobBiomass=2067 and CCI Biomass=871. Each circle represents an AGB bin and its size indicates the number of plot data while the whiskers correspond to the 25^{th} and 75^{th} quartile range of the map AGB.

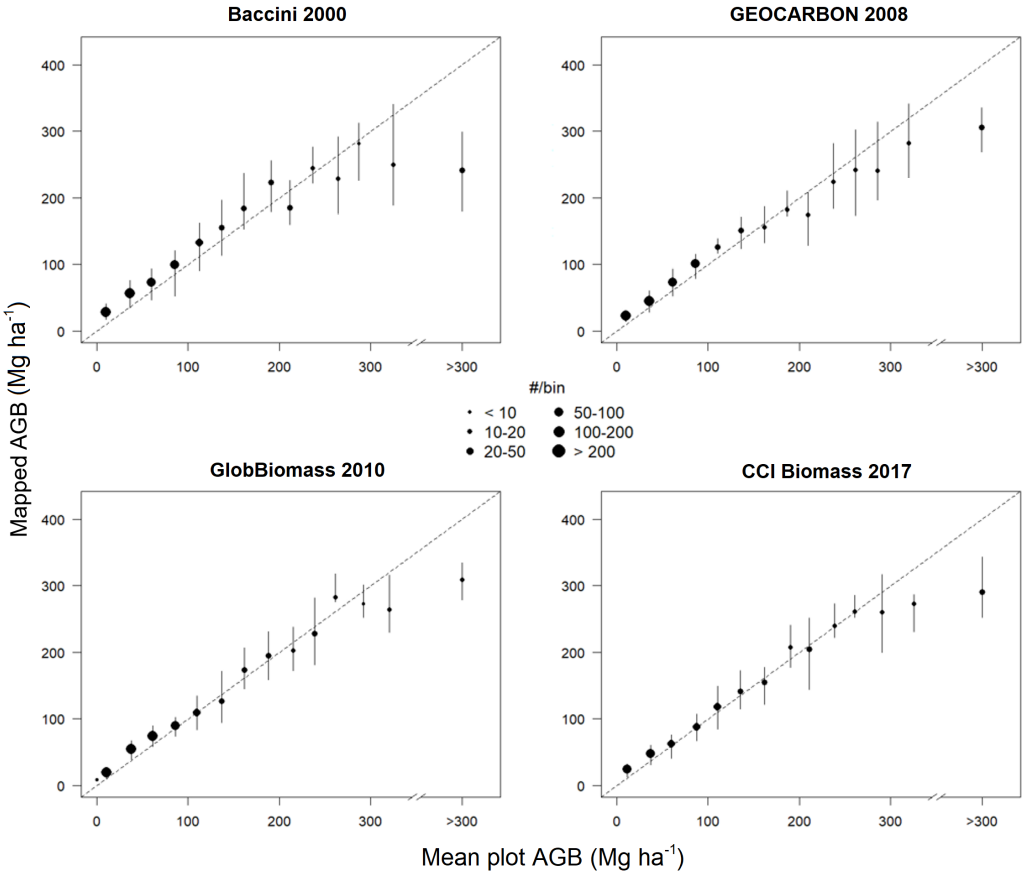

Fig. S5. Variogram models (VMs) fitted to data from the four AGB maps: (1) default VMs, (2) VMs adjusted by plot measurement error, and (3) convoluted VMs.

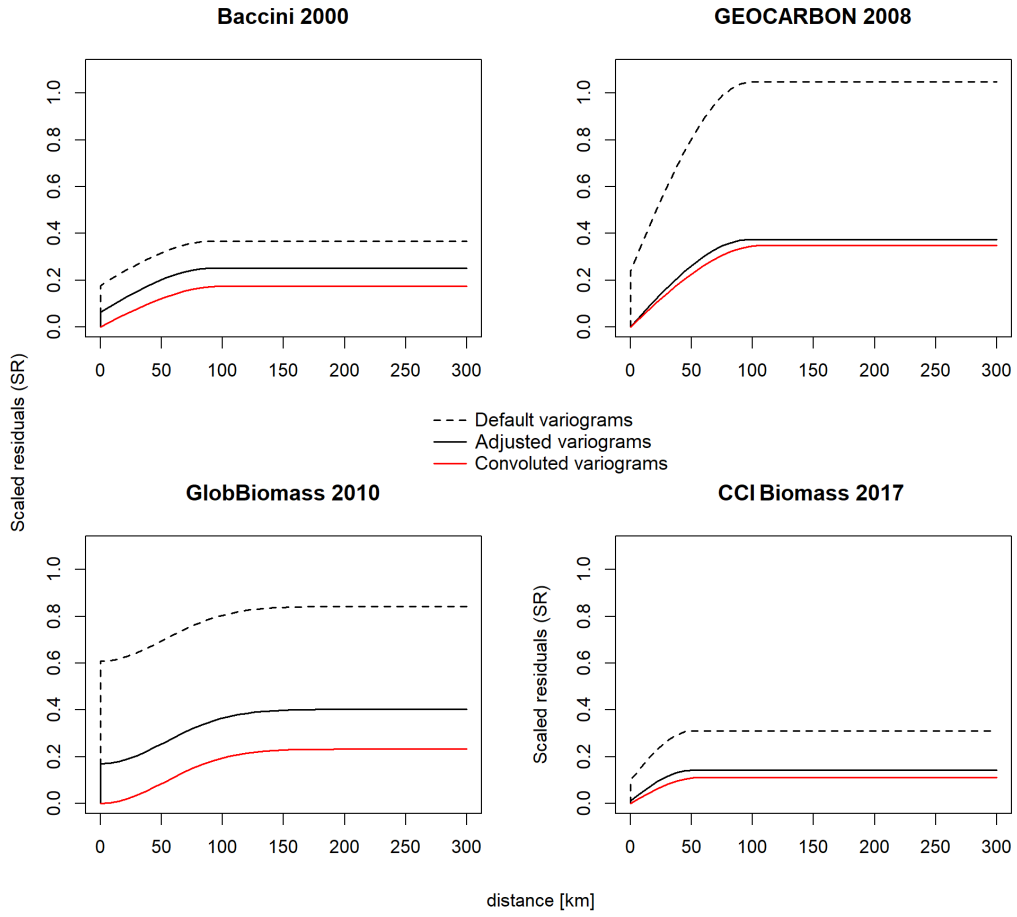

Fig. S6. The SD layers at original map pixel size (default SD) and the modified SD layers at 0.1° used for uncertainty aggregation in the pantropics. The modified maps account for spatial autocorrelation when averaging from original map resolution to 0.1°.

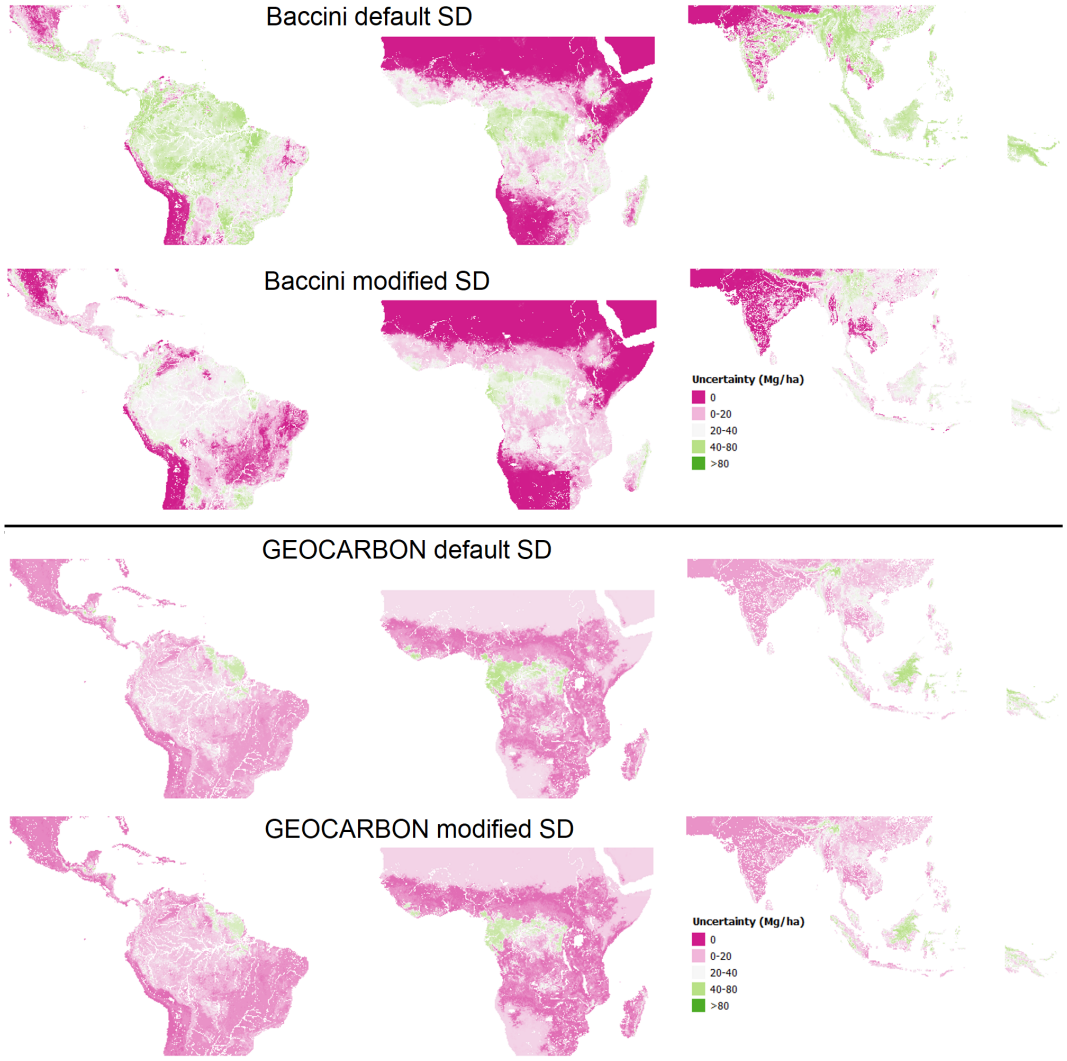

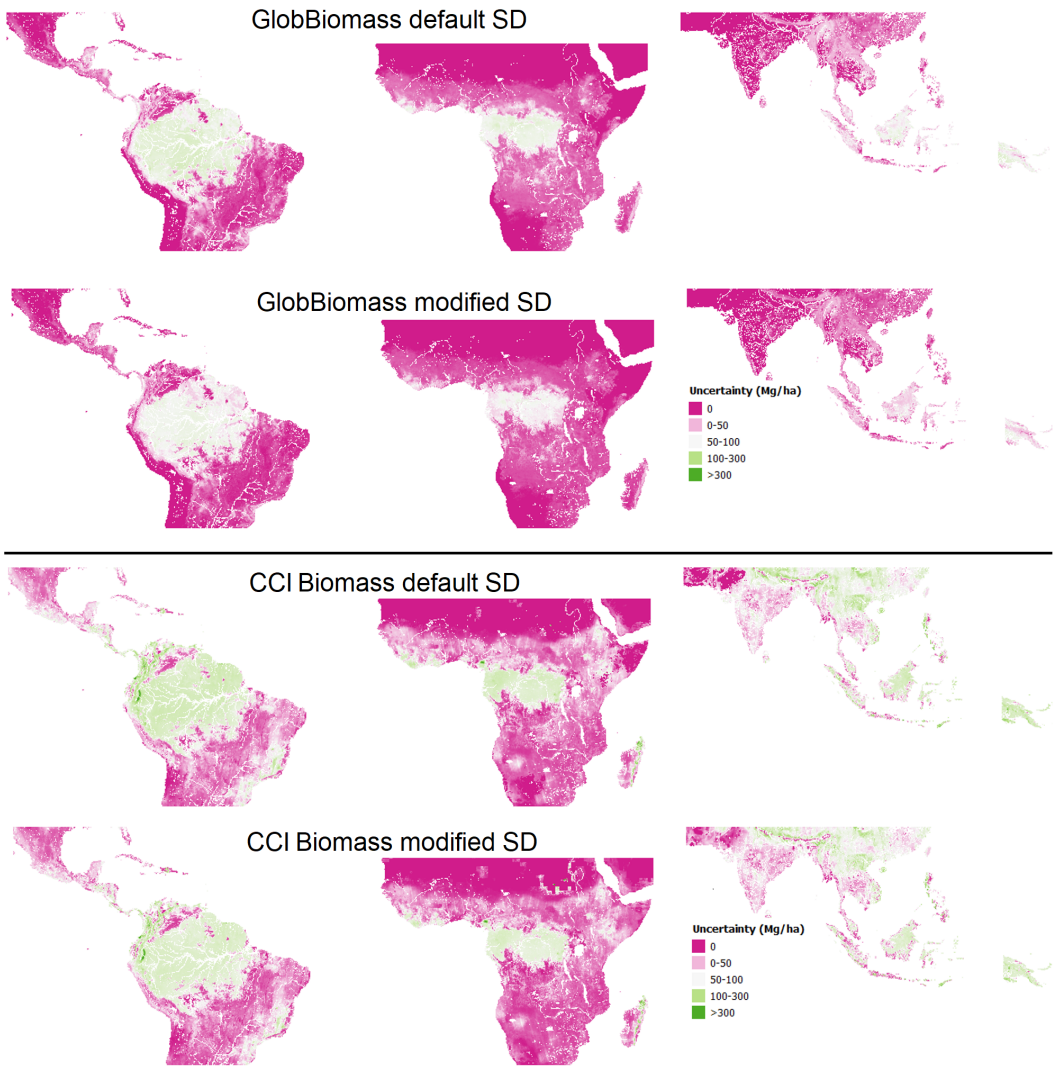

References

Araza, A., Herold, M., Hein, L., Quinones, M., 2021. The first aboveground biomass map of the philippines produced using remote sensing and machine learning, IEEE. https://doi.org/10.1109/igarss47720.2021.9553225, 10.1109/igarss47720.2021.9553225.

Auscover, T., 2016. Biomass plot library-national collation of tree and shrub inventory data, allometric model predictions of above and below-ground biomass, australia. Made available by the AusCover facility of the Terrestrial Ecosystem Research Network (TERN) .

Avitabile, V., Baccini, A., Friedl, M.A., Schmullius, C., 2012. Capabilities and limitations of landsat and land cover data for aboveground woody biomass estimation of uganda. Remote Sensing of Environment 117, 366–380. https://doi.org/10.1016/j.rse.2011.10.012.

Avitabile, V., Camia, A., 2018. An assessment of forest biomass maps in europe using harmonized national statistics and inventory plots. Forest Ecology and Management 409, 489–498. https://doi.org/10.1016/j.foreco.2017.11.047.

Avitabile, V., Herold, M., Heuvelink, G.B.M., Lewis, S.L., Phillips, O.L., Asner, G.P., Armston, J., Ashton, P.S., Banin, L., Bayol, N., Berry, N.J., Boeckx, P., de Jong, B.H.J., DeVries, B., Girardin, C.A.J., Kearsley, E., Lindsell, J.A., Lopez-Gonzalez, G., Lucas, R., Malhi, Y., Morel, A., Mitchard, E.T.A., Nagy, L., Qie, L., Quinones, M.J., Ryan, C.M., Ferry, S.J.W., Sunderland, T., Laurin, G.V., Gatti, R.C., Valentini, R., Verbeeck, H., Wijaya, A., Willcock, S., 2016. An integrated pan-tropical biomass map using multiple reference datasets. Global Change Biology 22, 1406–1420. https://doi.org/10.1111/gcb.13139.

Avitabile, V., Herold, M., Lewis, S., Phillips, O., Aguilar-Amuchastegui, N., Asner, G., Brienen, R., DeVries, B., Gazolla Gatti, R., Feldpausch, T., Girardin, C., de Jong, B., Kearsley, E., Klop, E., Lin, X., Lindsell, J., Lopez-Gonzalez, G., Lucas, R., Malhi, Y., Morel, A., Mitchard, E., Pandey, D., Piao, S., Ryan, C., Sales, M., Santoro, M., Vaglio Laurin, G., Valentini, R., Verbeeck, H., Wijaya, A., Willcock, S., 2014. Comparative analysis and fusion for improved global biomass mapping. pp. 251–252. `https://colloque6.inra.fr/gv2m/Oral-Sessions`.

Baccini, A., Goetz, S.J., Walker, W.S., Laporte, N.T., Sun, M., Sulla-Menashe, D., Hackler, J., Beck, P.S.A., Dubayah, R., Friedl, M.A., Samanta, S., Houghton, R.A., 2012. Estimated carbon dioxide emissions from tropical deforestation improved by carbon-density maps. Nature Climate Change 2, 182–185. https://doi.org/10.1038/nclimate1354.

Bispo, P.C., Santos, J.R., Valeriano, M.M., Touzi, R., Seifert, F.M., 2014. Integration of polarimetric PALSAR attributes and local geomorphometric variables derived from SRTM for forest biomass modeling in central amazonia. Canadian Journal of Remote Sensing 40, 26–42. https://doi.org/10.1080/07038992.2014.913477.

Brown, S., Goslee, K., Casarim, F., Harris, N., Petrova, S., 2014. Sampling design and implementation plan for guyana's redd+ forest carbon monitoring system (fcms): version 2. Submitted by Winrock International to the Guyana Forestry Commission .

Carreiras, J., Melo, J., Vasconcelos, M., 2013. Estimating the above-ground biomass in miombo savanna woodlands (mozambique, east africa) using l-band synthetic aperture radar data. Remote Sensing 5, 1524–1548. https://doi.org/10.3390/rs5041524.

Carreiras, J.M., Vasconcelos, M.J., Lucas, R.M., 2012. Understanding the relationship between aboveground biomass and ALOS PALSAR data in the forests of guinea-bissau (west africa). Remote Sensing of Environment 121, 426–442. https://doi.org/10.1016/j.rse.2012.02.012.

Chen, A., Peng, S., Fei, S., 2018. Mapping global forest biomass and its changes over the first decade of the 21st century. Science China Earth Sciences 62, 585–594. https://doi.org/10.1007/s11430-018-9277-6.

De Vries, B., Avitabile, V., Kooistra, L., Herold, M., 2012. Monitoring the impact of redd+ implementation in the unesco kafa biosphere reserve ethiopia. Sensing a Changing World .

Drichi, P., 2003. National Biomas Study of Uganda. Technical Report.

GlobalForestWatch, 2002. Global forest watch. World Resources Institute, Washington, DC. Available from http://www. globalforestwatch.org (accessed March 2020) .

Goodman, R.C., Phillips, O.L., del Castillo Torres, D., Freitas, L., Cortese, S.T., Monteagudo, A., Baker, T.R., 2013. Amazon palm biomass and allometry. Forest Ecology and Management 310, 994–1004. https://doi.org/10.1016/j.foreco.2013.09.045.

Hu, T., Su, Y., Xue, B., Liu, J., Zhao, X., Fang, J., Guo, Q., 2016. Mapping global forest aboveground biomass with spaceborne LiDAR, optical imagery, and forest inventory data 8, 565. https://doi.org/10.3390/rs8070565, 10.3390/rs8070565.

de Jong, B.H., 2013. Spatial distribution of biomass and links to reported disturbances in tropical lowland forests of southern mexico. Carbon Management 4, 601–615. https://doi.org/10.4155/cmt.13.60.

Kindermann, G., McCallum, I., Fritz, S., Obersteiner, M., 2008. A global forest growing stock, biomass and carbon map based on FAO statistics. Silva Fennica 42. https://doi.org/10.14214/sf.244.

Laurin, G.V., Hawthorne, W., Chiti, T., Paola, A.D., Gatti, R.C., Marconi, S., Noce, S., Grieco, E., Pirotti, F., Valentini, R., 2016. Does degradation from selective logging and illegal activities differently impact forest resources? a case study in ghana. iForest - Biogeosciences and Forestry 9, 354–362. https://doi.org/10.3832/ifor1779-008.

Lewis, S.L., Sonké, B., Sunderland, T., Begne, S.K., Lopez-Gonzalez, G., van der Heijden, G.M.F., Phillips, O.L., Affum-Baffoe, K., Baker, T.R., Banin, L., Bastin, J.F., Beeckman, H., Boeckx, P., Bogaert, J., Cannière, C.D., Chezeaux, E., Clark, C.J., Collins, M., Djagbletey, G., Djuikouo, M.N.K., Droissart, V., Doucet, J.L., Ewango, C.E.N., Fauset, S., Feldpausch, T.R., Foli, E.G., Gillet, J.F., Hamilton, A.C., Harris, D.J., Hart, T.B., de Haulleville, T., Hladik, A., Hufkens, K., Huygens, D., Jeanmart, P., Jeffery, K.J., Kearsley, E., Leal, M.E., Lloyd, J., Lovett, J.C., Makana, J.R., Malhi, Y., Marshall, A.R., Ojo, L., Peh, K.S.H., Pickavance, G., Poulsen, J.R., Reitsma, J.M., Sheil, D., Simo, M., Steppe, K., Taedoumg, H.E., Talbot, J., Taplin, J.R.D., Taylor, D., Thomas, S.C., Toirambe, B., Verbeeck, H., Vleminckx, J., White, L.J.T., Willcock, S., Woell, H., Zemagho, L., 2013. Above-ground biomass and structure of 260 african tropical forests. Philosophical Transactions of the Royal Society B: Biological Sciences 368, 20120295. https://doi.org/10.1098/rstb.2012.0295.

Liang, J., Zhou, M., Tobin, P.C., McGuire, A.D., Reich, P.B., 2015. Biodiversity influences plant productivity through niche–efficiency. Proceedings of the National Academy of Sciences 112, 5738–5743. https://doi.org/10.1073/pnas.1409853112.

Lindsell, J.A., Klop, E., 2013. Spatial and temporal variation of carbon stocks in a lowland tropical forest in west africa. Forest Ecology and Management 289, 10–17. 10.1016/j.foreco.2012.09.045.

Liu, Y.Y., van Dijk, A.I.J.M., de Jeu, R.A.M., Canadell, J.G., McCabe, M.F., Evans, J.P., Wang, G., 2015. Recent reversal in loss of global terrestrial biomass 5, 470–474. https://doi.org/10.1038/nclimate2581, 10.1038/nclimate2581.

Luyssaert, S., Schulze, E.D., Börner, A., Knohl, A., Hessenmöller, D., Law, B.E., Ciais, P., Grace, J., 2008. Old-growth forests as global carbon sinks. Nature 455, 213–215. https://doi.org/10.1038/nature07276.

Mitchard, E., Saatchi, S., Lewis, S., Feldpausch, T., Woodhouse, I., Sonké, B., Rowland, C., Meir, P., 2011. Measuring biomass changes due to woody encroachment and deforestation/degradation in a forest–savanna boundary region of central africa using multi-temporal l-band radar backscatter. Remote Sensing of Environment 115, 2861–2873. https://doi.org/10.1016/j.rse.2010.02.022.

Mitchard, E.T.A., Feldpausch, T.R., Brienen, R.J.W., Lopez-Gonzalez, G., Monteagudo, A., Baker, T.R., Lewis, S.L., Lloyd, J., Quesada, C.A., Gloor, M., ter Steege, H., Meir, P., Alvarez, E., Araujo-Murakami, A., Aragão, L.E.O.C., Arroyo, L., Aymard, G., Banki, O., Bonal, D., Brown, S., Brown, F.I., Cerón, C.E., Moscoso, V.C., Chave, J., Comiskey, J.A., Cornejo, F., Medina, M.C., Costa, L.D., Costa, F.R.C., Fiore, A.D., Domingues, T.F., Erwin, T.L., Frederickson, T., Higuchi, N., Coronado, E.N.H., Killeen, T.J., Laurance, W.F., Levis, C., Magnusson, W.E., Marimon, B.S., Junior, B.H.M., Polo, I.M., Mishra, P., Nascimento, M.T., Neill, D., Vargas, M.P.N., Palacios, W.A., Parada, A., Molina, G.P., Peña-Claros, M., Pitman, N., Peres, C.A., Poorter, L., Prieto, A., Ramirez-Angulo, H., Correa, Z.R., Roopsind, A., Roucoux, K.H., Rudas, A., Salomão, R.P., Schietti, J., Silveira, M., de Souza, P.F., Steininger, M.K., Stropp, J., Terborgh, J., Thomas, R., Toledo, M., Torres-Lezama, A., van Andel, T.R., van der Heijden, G.M.F., Vieira, I.C.G., Vieira, S., Vilanova-Torre, E., Vos, V.A., Wang, O., Zartman, C.E., Malhi, Y., Phillips, O.L., 2014. Markedly divergent estimates of amazon forest carbon density from ground plots and satellites. Global Ecology and Biogeography 23, 935–946. https://doi.org/10.1111/geb.12168.

Mitchard, E.T.A., Saatchi, S.S., Woodhouse, I.H., Nangendo, G., Ribeiro, N.S., Williams, M., Ryan, C.M., Lewis, S.L., Feldpausch, T.R., Meir, P., 2009. Using satellite radar backscatter to predict above-ground woody biomass: A consistent relationship across four different african landscapes. Geophysical Research Letters 36. https://doi.org/10.1029/2009gl040692.

Morel, A.C., Saatchi, S.S., Malhi, Y., Berry, N.J., Banin, L., Burslem, D., Nilus, R., Ong, R.C., 2011. Estimating aboveground biomass in forest and oil palm plantation in sabah, malaysian borneo using ALOS PALSAR data. Forest Ecology and Management 262, 1786–1798. https://doi.org/10.1016/j.foreco.2011.07.008.

Murdiyarso, D., Donato, D., Kauffman, J.B., Kurnianto, S., Stidham, M., Kanninen, M., 2009. Carbon storage in mangrove and peatland ecosystems: A preliminary account from plots in indonesia. Working paper 48. Bogor Banat, Indonesia: Center for International Forestry Research. 35 p. , 1–35.

Pacheco-Pascagaza, A.M., Garcia, M., Guez-Veiga, P.R., Balzter, H., 2018. The use of multifrequency sar data for assessing levels of forest disturbance in bajo calima colombia, in: IGARSS 2018-2018 IEEE International Geoscience and Remote Sensing Symposium, IEEE. pp. 7015–7018.

Ramesh, B., Venugopal, P.D., Pélissier, R., Patil, S.V., Swaminath, M., Couteron, P., 2010. Mesoscale patterns in the floristic composition of forests in the central western ghats of karnataka, india. Biotropica 42, 435–443.

Ruesch, A., Gibbs, H., 2008. New global biomass carbon map for the year 2000 based on ipcc tier-1 methodology. Oak Ridge National Laboratory's Carbon Dioxide Information Analysis Center: Oak Ridge, USA. Available online from the Carbon Dioxide Information Analysis Center, URL: http://cdiac. ornl. gov .

Saatchi, S.S., Harris, N.L., Brown, S., Lefsky, M., Mitchard, E.T.A., Salas, W., Zutta, B.R., Buermann, W., Lewis, S.L., Hagen, S., Petrova, S., White, L., Silman, M., Morel, A., 2011. Benchmark map of forest carbon stocks in tropical regions across three continents. Proceedings of the National Academy of Sciences 108, 9899–9904. https://doi.org/10.1073/pnas.1019576108.

Santoro, M., Beaudoin, A., Beer, C., Cartus, O., Fransson, J.E., Hall, R.J., Pathe, C., Schmullius, C., Schepaschenko, D., Shvidenko, A., Thurner, M., Wegmüller, U., 2015. Forest growing stock volume of the northern hemisphere: Spatially explicit estimates for 2010 derived from envisat ASAR. Remote Sensing of Environment 168, 316–334. https://doi.org/10.1016/j.rse.2015.07.005.

Santoro, M., Cartus, O., 2019. Esa biomass climate change initiative (biomass_cci): Global datasets of forest above-ground biomass for the year 2017, v1. https://doi.org/10.5285/BEDC59F37C9545C981A839EB552E4084.

Santoro, M., Cartus, O., Carvalhais, N., Rozendaal, D., Avitabilie, V., Araza, A., de Bruin, S., Herold, M., Quegan, S., Veiga, P.R., Balzter, H., Carreiras, J., Schepaschenko, D., Korets, M., Shimada, M., Itoh, T., Martínez, Á.M., Cavlovic, J., Gatti, R.C., da Conceição Bispo, P., Dewnath, N., Labrière, N., Liang, J., Lindsell, J., Mitchard, E.T.A., Morel, A., Pascagaza, A.M.P., Ryan, C.M., Slik, F., Laurin, G.V., Verbeeck, H., Wijaya, A., Willcock, S., 2020. The global forest aboveground biomass pool for 2010 estimated from high-resolution satellite observations https://doi.org/10.5194/essd-2020-148.

dos Santos, M., Keller, M., Morton, D., 2019. Lidar surveys over selected forest research sites, brazilian amazon, 2008-2018. https://doi.org/10.3334/ORNLDAAC/1644.

Schelhaas, M., Clerkx, A., Daamen, W., Oldenburger, J., Velema, G., Schnitger, P., Schoonderwoerd, H., Kramer, H., 2014. Zesde Nederlandse bosinventarisatie: methoden en basisresultaten. Technical Report. Alterra, Wageningen-UR.

Schepaschenko, D., Chave, J., Phillips, O.L., Lewis, S.L., Davies, S.J., Réjou-Méchain, M., Sist, P., Scipal, K., Perger, C., Herault, B., Labrière, N., Hofhansl, F., Affum-Baffoe, K., Aleinikov, A., Alonso, A., Amani, C., Araujo-Murakami, A., Armston, J., Arroyo, L., Ascarrunz, N., Azevedo, C., Baker, T., Bałazy, R., Bedeau, C., Berry, N., Bilous, A.M., Bilous, S.Y., Bissiengou, P., Blanc, L., Bobkova, K.S., Braslavskaya, T., Brienen, R., Burslem, D.F.R.P., Condit, R., Cuni-Sanchez, A., Danilina, D., del Castillo Torres, D., Derroire, G., Descroix, L., Sotta, E.D., d'Oliveira, M.V.N., Dresel, C., Erwin, T., Evdokimenko, M.D., Falck, J., Feldpausch, T.R., Foli, E.G., Foster, R., Fritz, S., Garcia-Abril, A.D., Gornov, A., Gornova, M., Gothard-Bassébé, E., Gourlet-Fleury, S., Guedes, M., Hamer, K.C., Susanty, F.H., Higuchi, N., Coronado, E.N.H., Hubau, W., Hubbell, S., Ilstedt, U., Ivanov, V.V., Kanashiro, M., Karlsson, A., Karminov, V.N., Killeen, T., Koffi, J.C.K., Konovalova, M., Kraxner, F., Krejza, J., Krisnawati, H., Krivobokov, L.V., Kuznetsov, M.A., Lakyda, I., Lakyda, P.I., Licona, J.C., Lucas, R.M., Lukina, N., Lussetti, D., Malhi, Y., Manzanera, J.A., Marimon, B., Junior, B.H.M., Martinez, R.V., Martynenko, O.V., Matsala, M., Matyashuk, R.K., Mazzei, L., Memiaghe, H., Mendoza, C., Mendoza, A.M., Morozuiuk, O.V., Mukhortova, L., Musa, S., Nazimova, D.I., Okuda, T., Oliveira, L.C., Ontikov, P.V., Osipov, A.F., Pietsch, S., Playfair, M., Poulsen, J., Radchenko, V.G., Rodney, K., Rozak, A.H., Ruschel, A., Rutishauser, E., See, L., Shchepashchenko, M., Shevchenko, N., Shvidenko, A., Silveira, M., Singh, J., Sonké, B., Souza, C., Stereńczak, K., Stonozhenko, L., Sullivan, M.J.P., Szatniewska, J., Taedoumg, H., ter Steege, H., Tikhonova, E., Toledo, M., Trefilova, O.V., Valbuena, R., Gamarra, L.V., Vasiliev, S., Vedrova, E.F., Verhovets, S.V., Vidal, E., Vladimirova, N.A., Vleminckx, J., Vos, V.A., Vozmitel, F.K., Wanek, W., West, T.A.P., Woell, H., Woods, J.T., Wortel, V., Yamada, T., Hajar, Z.S.N., Zo-Bi, I.C., 2019. The forest observation system, building a global reference dataset for remote sensing of forest biomass. Scientific Data 6. https://doi.org/10.1038/s41597-019-0196-1.

Slik, J.W.F., Paoli, G., McGuire, K., Amaral, I., Barroso, J., Bastian, M., Blanc, L., Bongers, F., Boundja, P., Clark, C., Collins, M., Dauby, G., Ding, Y., Doucet, J.L., Eler, E., Ferreira, L., Forshed, O., Fredriksson, G., Gillet, J.F., Harris, D., Leal, M., Laumonier, Y., Malhi, Y., Mansor, A., Martin, E., Miyamoto, K., Araujo-Murakami, A., Nagamasu, H., Nilus, R., Nurtjahya, E., Oliveira, Á., Onrizal, O., Parada-Gutierrez, A., Permana, A., Poorter, L., Poulsen, J., Ramirez-Angulo, H., Reitsma, J., Rovero, F., Rozak, A., Sheil, D., Silva-Espejo, J., Silveira, M., Spironelo, W., ter Steege, H., Stevart, T., Navarro-Aguilar, G.E., Sunderland, T., Suzuki, E., Tang, J., Theilade, I., van der Heijden, G., van Valkenburg, J., Do, T.V., Vilanova, E., Vos, V., Wich, S., Wöll, H., Yoneda, T., Zang, R., Zhang, M.G., Zweifel, N., 2013. Large trees drive forest aboveground biomass variation in moist lowland forests across the tropics. Global Ecology and Biogeography 22, 1261–1271. https://doi.org/10.1111/geb.12092.

Vieilledent, G., Gardi, O., Grinand, C., Burren, C., Andriamanjato, M., Camara, C.,

Gardner, C.J., Glass, L., Rasolohery, A., Ratsimba, H.R., Gond, V., Rakotoarijaona, J.R., 2016. Bioclimatic envelope models predict a decrease in tropical forest carbon stocks with climate change in madagascar. Journal of Ecology 104, 703–715. https://doi.org/10.1111/1365-2745.12548.

Wijaya, A., Liesenberg, V., Susanti, A., Karyanto, O., Verchot, L.V., 2015. Estimation of biomass carbon stocks over peat swamp forests using multi-temporal and multi-polratizations SAR data. ISPRS - International Archives of the Photogrammetry, Remote Sensing and Spatial Information Sciences XL-7/W3, 551–556. https://doi.org/10.5194/isprsarchives-xl-7-w3-551-2015.

Willcock, S., Phillips, O.L., Platts, P.J., Balmford, A., Burgess, N.D., Lovett, J.C., Ahrends, A., Bayliss, J., Doggart, N., Doody, K., Fanning, E., Green, J.M., Hall, J., Howell, K.L., Marchant, R., Marshall, A.R., Mbilinyi, B., Munishi, P.K., Owen, N., Swetnam, R.D., Topp-Jorgensen, E.J., Lewis, S.L., 2014. Quantifying and understanding carbon storage and sequestration within the eastern arc mountains of tanzania, a tropical biodiversity hotspot. Carbon Balance and Management 9. https://doi.org/10.1186/1750-0680-9-2.

Yang, L., Liang, S., Zhang, Y., 2020. A new method for generating a global forest aboveground biomass map from multiple high-level satellite products and ancillary information. IEEE Journal of Selected Topics in Applied Earth Observations and Remote Sensing 13, 2587–2597. https://doi.org/10.1109/jstars.2020.2987951.

Zhang, Y., Liang, S., 2020. Fusion of multiple gridded biomass datasets for generating a global forest aboveground biomass map. Remote Sensing 12, 2559. https://doi.org/10.3390/rs12162559.

Zhang, Y., Liang, S., Yang, L., 2019. A review of regional and global gridded forest biomass datasets. Remote Sensing 11, 2744. https://doi.org/10.3390/rs11232744.